Available online at www.sciencedirect.com
ScienceDirect
Composites Science and Technology 68 (2008) 164–170
COMPOSITES SCIENCE AND TECHNOLOGY
www.elsevier.com/locate/compscitech

Strengthening and thermal stabilization of polyurethane nanocomposites with silicon carbide nanoparticles by a surface-initiated-polymerization approach

Zhanhu Guo *, Ta Y. Kim, Kenny Lei, Tony Pereira, Jonathan G. Sugar, H. Thomas Hahn

Mechanical and Aerospace Engineering Department and Materials Science and Engineering Department, University of California Los Angeles, Los Angeles, CA 90095, United States

Received 20 February 2007; received in revised form 26 April 2007; accepted 8 May 2007
Available online 25 May 2007

Abstract

Silicon carbide reinforced polyurethane nanocomposites were fabricated by a facile surface-initiated-polymerization (SIP) method. The particle loading was tuned to up to 35 wt% without any obvious shrinkage and breakage as compared with the conventional direct mixing method. An increased thermal stability of the composites was observed with the addition of the silicon carbide nanoparticles under thermo-gravimetric analysis (TGA). Tensile strength was observed to increase dramatically with the increase of the particle loading. Both the uniform particle dispersion and the strong chemical bonding between the nanoparticles and the polymer–matrix contributed to the enhanced thermal stability and improved mechanical properties.

Keywords: A. Particle-reinforced composites; A. Polymer–matrix composites (PMCs); B. Mechanical properties; A. Structural materials

1. Introduction

Incorporation of functional nanoparticles into a polymer–matrix has spurred much interest due to their cost-effective processability, special physical properties such as increased electric/heat conductivities [1,2], enhanced stiffness and strength [3], improved shape replicability [4] and high-flexibility, which render possible many applications such as microwave absorbers [5–7], photovoltaic (solar) cells [8,9], and smart structures [10,11]. The reported methods for the polymeric nanocomposite fabrication include *ex situ* methods, i.e., dispersion of the synthesized nanoparticles into a polymeric solution [12–14], *in situ* monomer polymerization methods in the presence of the nanoparticles [15–19], or *in situ* formation of nanoparticles in the presence of the polymer [20]. The interactions between the polymer and the nanoparticles for the *ex situ* formed composites are normally steric interaction forces, van der Waals forces, or Lewis acid–base interactions. However, *in situ* synthesis methods can create strong chemical bonding within the nanocomposites and are expected to produce more-stable and higher-quality nanocomposites [12–14].

The existing challenge in the composite fabrication is to provide a sufficiently high tensile strength due to local stress within the nanocomposite. In other words, the response of a material to an applied stress is strongly dependent on the nature of the bonds. The interfacial interactions between nanoparticles and polymer–matrix play a crucial role in the local stress transfer and determining the quality and properties of the nanocomposites [12–14]. The poor bonding linkage between the fillers and the polymer–matrix will introduce artificial defects, which consequently result in a deleterious effect on the mechanical properties of the nanocomposites [21]. Introducing good linkages between the nanoparticles and the polymer–matrix is still a challenge for specific composite fabrication. However, appropriate chemical engineering treatment

* Corresponding author. Tel.: +1 310 206 8157.
E-mail address: zhanhu@seas.ucla.edu (Z. Guo).

0266-3538/$ - see front matter © 2007 Elsevier Ltd. All rights reserved.
doi:10.1016/j.compscitech.2007.05.031

(functionalization) of the nanofiller surface by introducing proper functional groups could improve both the strength and toughness of the subsequent composites with improved compatibility between the nanofillers and the polymer–matrix [3], and make the nanocomposites stable in harsh environments as well [3,22]. Thus, surface functionalization of nanoparticles with a surfactant or a coupling agent is important not only to stabilize the nanoparticles [23] during processing but also to render them compatible with the polymer–matrix.

Silicon carbide, a well known ceramic material, has unique physical properties such as superior resistance to chemicals and high-temperature, high-electron mobility, excellent thermal/heat conductivity and superior mechanical properties [24,25], which permit possible various applications such as nanodevices in harsh environments. Polyurethane is chosen in this research due to its wide applications such as in the coating industry and shape memory devices under application of an external stimulus such as thermal heating, electric heating, magnetic field or chemicals. Recently, we have demonstrated the usage of a bi-functional coupling agent, methacryloxypropyltrimethoxysilane (MPS), for the functionalization of the ceramic nanoparticles including alumina, zinc oxide and copper oxide to improve the chemical interaction between the nanoparticles and the polymer–matrix [3,26,27]. The uniform particle dispersion and the strong chemical interaction between nanoparticles and the polymer–matrix were observed. As a result, the tensile strength of the vinyl-ester resin nanocomposites was enhanced significantly and strongly depended on the nature and the concentration of the nanofillers.

In this paper, we report on the processing and characterization of a particulate nanocomposite that consists of silicon carbide nanoparticles dispersed in a polymer–matrix. No additional surfactant or coupling agent was needed for the particle functionalization. The present hydrolyzed –OH groups provide a bridging between the nanoparticle and the polymer–matrix through the polymerization. Tensile tests revealed a dramatic increase in the tensile strength arising from the strong chemical bonding and the uniform particle dispersion.

2. Experimental

2.1. Materials

Spherical silicon carbide nanoparticles (SiC with a purity of >98%, specific surface area: 70–90 m^2/g; β-SiC majority phase) with a size of about 30 nm were purchased from MTI corporation. The chemical structures of the two-part urethane monomers (diisocyanate and diol, CAAP-COAT FP-002-55X, CAAP Co., Inc.) are shown in Chart 1. All the chemicals were used as-received without further treatment.

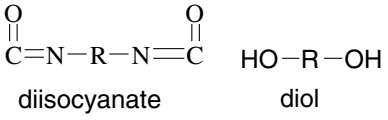

Chart 1. Chemical formulas of the two-part polyurethane monomers used.

2.2. Nanocomposite fabrication

The surface-initiated-polymerization (SIP) method [28–30] allows a high-loading, up to 35 wt%, of SiC nanoparticles to be incorporated into the polyurethane matrix. In the SIP method, both the catalyst (a liquid containing aliphatic amine, parachlorobenzotrifluoride and methyl propyl ketone) and the accelerator (polyurethane STD-102, containing organo-titanate) are added drop by drop within half hour into a silicon carbide nanoparticle suspended tetrahydrofuran solution and sonicated for an additional half hour. The two-part monomers of diisocyanate and diol are introduced into the above solution to polymerize for 6 h, and then poured into a mold for solvent evaporation. The conventional direct mixing (DM) method used for the microparticle reinforced composites fabrication was carried out by adding the nanoparticles into a mixture of urethane monomer, catalyst, and accelerator in a tetrahydrofuran solution. The suspended solution was ultrasonically stirred for 5 min and then poured into a mold for curing and solvent evaporation. All the operations were carried out with ultrasonication. Nanocomposites with different particle loadings of 5 wt%, 20 wt% and 35 wt% were fabricated by the DM and SIP method, respectively.

2.3. Characterization

Particle structures were characterized on a JEOL transmission electron microscope (TEM, JEOL TEM-2010). FT-IR spectra were recorded in a Fourier transform infrared spectrometer (Jasco, FT-IR 420) in transmission mode under dried nitrogen flow (10 cubic centimeters per minute, cm^3/min, ccpm) condition. The as-received nanoparticles were mixed with powder KBr, ground and compressed into a pellet. The dispersion quality of the nanoparticle in the cured polyurethane matrix was investigated by a field emission scanning electron microscope (SEM) on the polished nanocomposite crosssectional area. The SEM samples were carefully prepared as follows. The cured SiC/polyurethane nanocomposite samples were embedded into a vinyl-ester resin tab, polished with a 1000-grit sand paper and a following 50 nm alumina nanoparticle aqueous solution polishing to achieve a smooth surface, then washed with DI water. This was followed by sputter coating a thin gold layer about 3 nm thick on the dried sample for SEM observation. The weight percentage of nanoparticles in the nanocomposites was determined by the thermogravimetric analysis (TGA, PerkinElmer) with an argon flow rate of 50 ccpm.

The mechanical properties of the fabricated nanocomposites were evaluated by tensile tests following the American Society for Testing and Materials (ASTM, 2002, standard D 412-98a) standard. An Instron 4411 with Series IX software testing machine was used. The samples were prepared according to the standard procedures. A crosshead speed of 25 mm/min was used and strain (mm/mm) was calculated by dividing the crosshead displacement by the gage length.

The samples for fracture mechanism study of the nanocomposites were prepared by solidifying the flexible composites with liquid nitrogen and breaking by hand. For better SEM image observation, the fracture surfaces were coated with a thin gold layer of 3 nm thickness.

3. Results and discussion

Fig. 1 shows the TEM bright field microstructures of the as-received silicon carbide nanoparticles. The obvious contrast within the particle in Fig. 1 is due to the oxidation of the silicon carbide nanoparticle surface causing the core-shell like structure. The contrast characteristic of the white parallel lines within the particles is due to the stacking faults [31]. The lattice distance of 0.251 nm (ring 1), 0.215 nm (ring 2), 0.1255 nm (ring 5), 0.110 nm (ring 6) and 0.100 nm (ring 7) of the selected area electron diffraction (SAED) shown in the inset of Fig. 1 can be assigned to (111), (200), (222), (400) and (331) planes of silicon carbide (Standard XRD file: PDF#29-1129); 0.175 nm (ring 3) and 0.143 nm (ring 4) arise from the (220) and (312) planes of silicon oxide, respectively (Standard XRD file: PDF#39-1425). This indicates that silicon has been partially oxidized on the silicon carbide nanoparticle surface with the formation of the crystalline silicon oxide, which could have happened during the silicon carbide formation at high-temperature and is consistent with the crystalline silicon oxide formation at high-temperature oxidation of the silicon [32,33]. Fourier-transform infrared (FT-IR) spectroscopic study also verified the formation of silicon oxide and further indicates the presence of hydrolyzed silicon oxide [34].

Fig. 2 shows the optical microstructures of the composites with a particle loading of 20 wt% fabricated by the surface-initiated-polymerization (SIP) method and the conventional direct mixing (DM) method, respectively. Large cracks were observed in the nanocomposites fabricated by conventional direct mixing method as shown in Fig. 2b; whereas no visible sign of cracking was observed in the nanocomposites fabricated by the surface-initiated-polymerization method, especially in the high-particle loading. Based on the fact that the high-quality nanocomposites were fabricated by the SIP method, as compared with the brittleness and obvious breakage of nanocomposites from the DM method, only SIP nanocomposite samples were used in the subsequent tests.

Fig. 3 shows the SEM microstructures of the SIP nanocomposites with particle loading of 5 wt% and 35 wt%, respectively. The samples were prepared by polishing with 1000-grit sand paper and 50 nm alumina nanoparticles to study the particle distribution within the polyurethane matrix in the interior of the composites. No obvious particle agglomeration was observed in the polymer–matrix even in the high-particle loading of 35 wt% indicating that SIP favors forming high-quality composites.

The thermal stability of the pure polyurethane and nanocomposites with different loadings was studied by thermo-gravimetric analysis (TGA, Perkin–Elmer) with an argon flow rate of 50 ccpm. Fig. 4 shows the weight percentage change as a function of temperature. The addition of silicon carbide nanoparticles makes the polyurethane more stable with a higher initiate decomposition and complete decomposition temperature. The pure polyurethane decomposed completely at temperatures higher than 550 °C and the different plateau level of the composite species is arising from the particle loading difference. When the nanoparticles were added, the decomposition temperature was observed to increase slightly. This is due to the retarding effect of the silicon carbide nanoparticles on the movement of the polyurethane chains considering the inert nature of the silicon carbide, which has also been observed

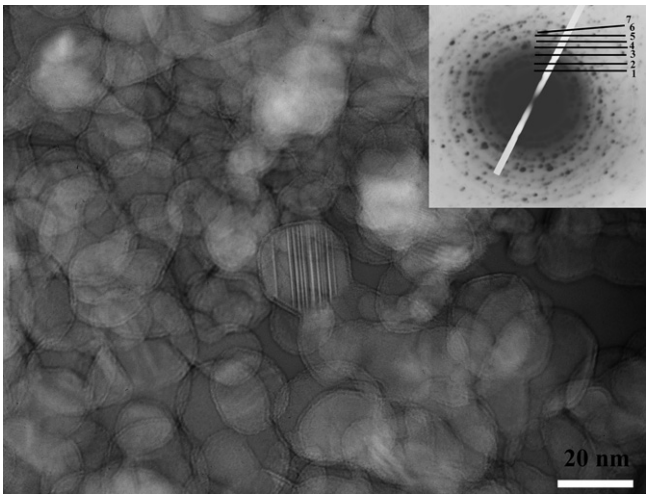

Fig. 1. Bright field TEM microstructure and SAED of the nanoparticles.

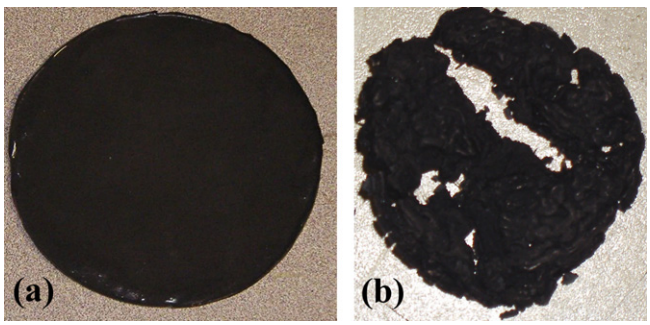

Fig. 2. Photograph of the composites fabricated by (a) SIP method and (b) DM method.

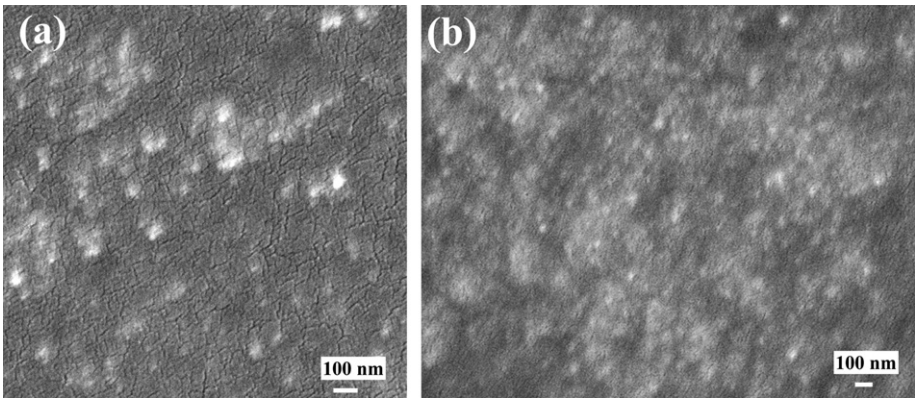

Fig. 3. SEM micrographs of the SIP nanocomposites with a loading of (a) 5 wt% and (b) 35 wt%, respectively.

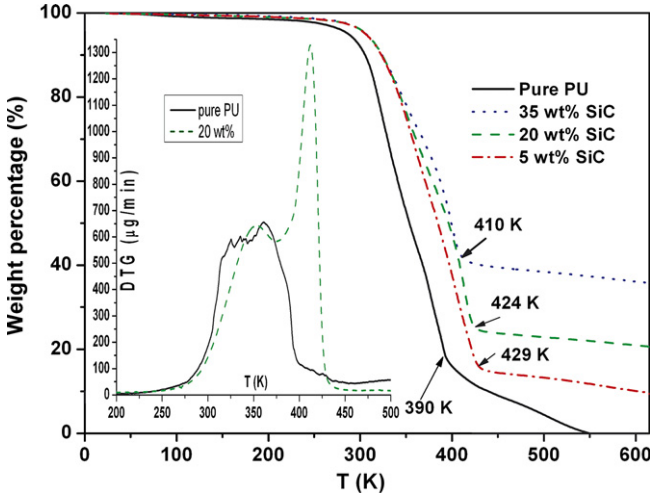

Fig. 4. TGA of the nanocomposites with different loadings; inset shows the derivative thermal gravimetric curve of pure polyurethane and the nanocomposites with a particle loading of 20 wt%.

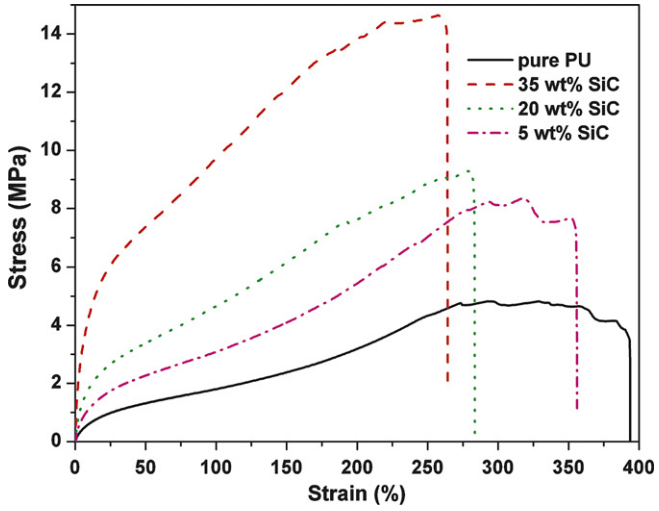

Fig. 5. Tensile stress versus strain curves of nanocomposites at different loadings.

in the multi-walled carbon nanotube (MWCNT) reinforced polybenzoxazine nanocomposites [35].

Derivative thermal gravimetric (DTG) was further used to study the thermal stability of the nanocomposites as compared with the pure polyurethane, which can shed some light on the chemical structure of the SIP nanocomposites. Different thermal behavior was observed with the addition of the silicon carbide nanoparticles into the polyurethane. As compared with the only peak presented in the cured pure polyurethane, two peaks were observed in the nanocomposites as shown in the inset of Fig. 4. The first peak is attributed to the bulk polyurethane matrix and the second peak at higher temperature is due to the polyurethane physicochemically attached to the nanoparticle surface. This phenomenon indicates a strong chemical bonding between the nanoparticles and the polyurethane matrix.

The effect of the interfacial interaction on the mechanical properties was investigated by tensile tests. Fig. 5 shows the typical tensile stress–strain curves of the pure polyurethane and nanocomposites with different loadings. The addition of SiC nanoparticles is seen to increase both the strength and the modulus together with an enhanced toughness. The mechanical properties of the neat cured polyurethane and nanocomposites with different loading are summarized in Table 1. As compared with the pure polyurethane, the addition of 5 wt% silicon carbide nanoparticles increases the Young's modulus and strength by a factor of 71% and 166%, respectively. The sacrificing loss of elongation is about 17%. An increase of about 21.4 times and 2.2 times in the modulus and strength, respectively, was observed in the composites reinforced with 35 wt%

Table 1
Mechanical properties of the pure polyurethane and nanocomposites with different loadings

	Modulus (MPa)	Strength (MPa)	Elongation (%)
Pure polyurethane	4.3 ± 0.8	3.7 ± 1.0	441.7 ± 86.4
Composite 5 wt%	11.5 ± 3.2	6.3 ± 1.0	366.6 ± 64.0
Composite 20 wt%	21.1 ± 4.8	7.4 ± 1.7	295.4 ± 65.8
Composite 35 wt%	96.2 ± 16.1	11.9 ± 2.3	225.5 ± 29.9

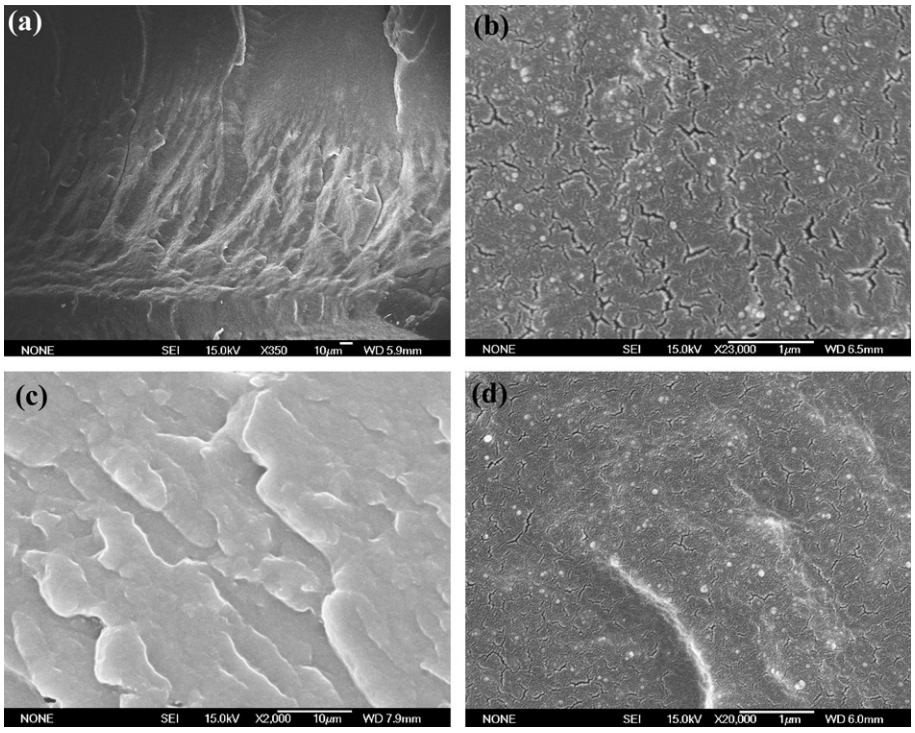

Fig. 6. SEM fracture surface microstructures of nanocomposites with a particle loading of (a), (b) 5 wt% and (c), (d) 35 wt%, respectively.

nanoparticles as compared with the pure polyurethane. The Young's modulus and strength is much larger than that of 20 wt% silicon carbide/polyurethane nanocomposites (3.9 times and 0.98 times in the modulus and strength, respectively).

SEM was used to study the fracture surface of the nanocomposites with different particle loading. The samples were prepared by breaking the liquid-nitrogen-frozen SiC/polyurethane nanocomposites and a thin gold coating was applied to improve the conductivity for good image observation. No agglomerated nanoparticles were observed in the fracture surface as seen in Fig. 6 indicating that the fracture was not due to the agglomerated nanoparticles, which could serve as microparticle like defects within poor composites and have a deleterious effect on the mechanical properties. However, the observed discrete nanoparticles without obvious agglomeration indicate a uniform dispersion in the nanocomposites fabricated by the SIP method. The images with high-magnification shown in Fig. 6b and d of the nanocomposites show particles with different size. This is due to the particles embedding at different depths in the polyurethane matrix. No void/holes arising from the possible peeling off the nanoparticles from the polymer–matrix were observed, which indicates a strong chemical interaction between the nanoparticles and polyurethane matrix. The strong interfacial interactions between the nanoparticles and the polyurethane matrix thus have an important effect on the effective transfer of the local stress. The extremely higher specific surface area inherent with the nanoscale particles as compared with the microparticles together with the strong interfacial chemical bonding between the polymer–matrix and the reinforcing nanoparticles effectively facilitate the local stress transfer into the tougher silicon carbide nanoparticles, which results in a much higher tensile strength as compared with the cured pure polyurethane. Chart 2 shows the nanocomposite fabrication through the SIP approach, illustrating the interaction between the nanoparticles and the polymer–matrix.

As compared with the recent report on the silicon carbide nanoparticles reinforced epoxy resin nanocomposites with a maximum loading of 1 wt% for the fabrication of

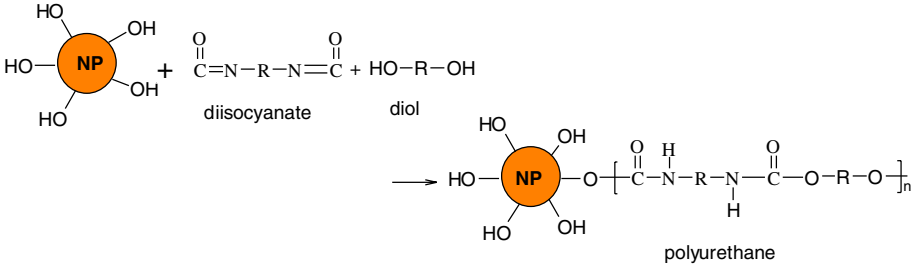

Chart 2. Scheme of the nanocomposite formation by the SIP method.

the strongest nanocomposite [36], the 35 wt% loading obtained here is much higher and does not show any deleterious effect on the tensile strength. The only drawback is a decrease in tensile strain. Considering the SIP method adopted here, the urethane monomers react with the hydrolyzed SiC nanoparticles, preventing the agglomeration of the nanoparticles due to steric forces. The strong chemical bonding between the nanoparticles and the polymer matrix, and the uniform dispersion of the nanoparticles favor the higher tensile strength. The microparticles arising from the nanoparticle agglomeration were regarded as a major factor in decreasing the tensile strength of the SiC nanoparticle reinforced epoxy resin nanocomposites [36].

4. Conclusion

Polyurethane nanocomposites reinforced with silicon carbide nanoparticles were synthesized using the SIP method. As compared with the conventional direct mixing method, the fabricated flexible SiC/polyurethane nanocomposites are significantly strengthened and have an improved thermal stability. The tensile tests revealed a strengthened structural nanomaterial and the tensile strength was observed to increase by 2.2 times higher than that of the cured pure polyurethane. Most importantly, the nanoparticle loading is much higher than what is possible when the nanocomposites are fabricated by the conventional DM method. The SIP method could be a standard approach for nanocomposite preparation especially with high-particle loading, which is necessary for certain applications such as giant magnetoresistance (GMR) sensors [37], microwave absorbers [38], proton-exchange membranes (PEM) used in fuel cells, and solar cells.

Acknowledgements

This work was partially supported by the Air Force Office of Scientific Research through AFOSR Grant FA9550-05-1-0138 with Dr. B. Les Lee as the Program Manager. Z. Guo kindly acknowledges the support from the UC-Discovery Grant ELE06-10268 and QuantumSphere research grant (QuantumSphere Inc.). The FT-IR spectroscopy, TGA and SEM were done in the MCTP lab which is supported by the NSF IGERT Materials Creation Training Program under Grant DGE-0114443.

References

[1] Stankovich S, Dikin DA, Dommett GHB, Kohlhaas KM, Zimney EJ, Stach EA, et al. Graphene-based composite materials. Nature 2006;442:282–6.
[2] Huang MT, Choi O, Ju YS, Hahn HT. Heat conduction in graphite-nanoplatelet-reinforced polymer nanocomposites. Appl Phys Lett 2006;89:023117/1–7/3.
[3] Guo Z, Pereira T, Choi O, Wang Y, Hahn HT. Surface functionalized alumina nanoparticle filled polymeric nanocomposites with enhanced mechanical properties. J Mater Chem 2006;16:2800–8.
[4] Sozzani P, Bracco S, Comotti A, Simonutti R, Valsesia P, Sakamoto Y, et al. Complete shape retention in the transformation of silica to polymer micro-objects. Nat Mater 2006;5:545–51.
[5] Sareni B, Krahenbuhl L, Beroual A, Brosseau C. Complete effective permittivity of a lossy composite material. J Appl Phys 1996;80: 4560–5.
[6] Brosseau C, Queffelec P, Talbot P. Microwave characterization of filled polymers. J Appl Phys 2001;89:4532–40.
[7] Liu J, Itoh M, Machida KI. Magnetic and electromagnetic wave absorption of a a-Fe/Z-type Ba-ferrite nanocomposites. Appl Phys Lett 2006;88:062503.
[8] Yu G, Gao J, Hummelen JC, Wudl F, Heeger AJ. Polymer photovoltaic cells: enhanced efficiencies via a network of internal donor–acceptor heterojunctions. Science 1995;270:1789–91.
[9] Beek WJE, Wienk MM, Jassen RAJ. Efficient hybrid solar cells from zinc oxide nanoparticles and a conjugated polymer. Adv Mater 2004;16:1009–13.
[10] Koerner H, Price G, Pearce NA, Alexander M, Vaia RA. Remotely actuated polymer nanocomposites stress-recovery of carbon-nanotube-filled thermoplastic elastomers. Nat Mater 2004;3:115–20.
[11] Mohr R, Kratz K, Weigel T, Lucka-Gabor M, Moneke M, Lendlein A. Initiation of shape-memory effect by inductive heating of magnetic nanoparticles in thermoplastic polymers. Proc Natl Acad Sci 2006;103:3540–5.
[12] Mammeri F, Bourhis EL, Rozes L, Sanchez C. Mechanical properties of hybrid organic–inorganic materials. J Mater Chem 2005;15: 3787–811.
[13] Sanchez C, Ribot F. Design of hybrid organic–inorganic materials synthesized via sol–gel chemistry. New J Chem 1994;18:1007–47.
[14] Judeinstein P, Sanchez C. Hybrid organic–inorganic materials: A land of multidisciplinary. J Mater Chem 1996;6:511–25.
[15] Marutani E, Yamamoto S, Ninjbadgar T, Tsujii Y, Fukuda T, Takano M. Surface-initiated atom transfer radical polymerization of methyl methacrylate on magnetite nanoparticles. Polymer 2004;45: 2231–5.
[16] Yu S, Chow GM. Carboxyl group (–CO_2H) functionalized ferrimagnetic iron oxide nanoparticles for potential bioapplications. J Mater Chem 2004;14:2781–6.
[17] Wilson JL, Poddar P, Frey NA, Srikanth H, Mohomed K, Harmon JP, et al. Synthesis and magnetic properties of polymer nanocomposites with embedded iron nanoparticles. J Appl Phys 2004;95: 1439–43.
[18] Xu X, Friedman G, Humfeld KD, Majetich SA, Asher SA. Synthesis and utilization of monodisperse superparamagnetic colloidal particles for magnetically controllable photonic crystals. Chem Mater 2002;14:1249–56.
[19] Fang J, Tung LD, Stokes KL, He J, Caruntu D, Zhou WL, et al. Synthesis and magnetic properties of CoPt-poly(methyl methacrylate) nanostructured composite material. J Appl Phys 2002;91:8816–8.
[20] Guo Z, Henry LL, Palshin V, Podlaha EJ. Synthesis of poly(methyl methacrylate) stabilized colloidal zero-valence metallic nanoparticles. J Mater Chem 2006;16:1772–7.
[21] Zhang X, Simon LC. In situ polymerization of hybrid polyethylene–alumina nanocomposites. Macromol Mater Eng 2005;290:573–83.
[22] Gao SL, Mader E. Characterization of interphase nanoscale property variations in glass fibre reinforced polypropylene and epoxy resin composites. Composites 2002;33A:559–76.
[23] Shenhar R, Norsten TB, Rotello VM. Polymer-mediated nanoparticle assembly: Structural control and applications. Adv Mater 2005;17:657–69.
[24] Zhou W, Liu X, Zhang Y. Simple approach to SiC nanowires: Synthesis, optical and electrical properties. Appl Phys Lett 2006;89: 223124.
[25] Monroy E, Ommes F, Calle F. Wide-bandgap semiconductor ultraviolet photodectors. Semicond Sci Technol 2003;18:R33–51.
[26] Guo Z, Wei S, Shedd B, Scaffaro R, Pereira T, Hahn HT. Particle surface engineering effect on the mechanical, optical and photoluminescent properties of ZnO/vinyl-ester resin nanocomposites. J Mater Chem 2007;17:806–13.
[27] Guo Z, Liang X, Pereira T, Scaffaro R, Hahn HT. CuO nanoparticle filled vinyl-ester resin nanocomposites: Fabrication, character-

ization and property analysis. Compos Sci Technol 2007;67: 2036–44.
[28] Advincula RC. Surface initiated polymerization from nanoparticle surfaces. J Dispersion Sci Technol 2003;24:343–61.
[29] Jennings GK, Brantley EL. Physicochemical properties of surface-initiated polymer films in the modification and processing of materials. Adv Mater 2004;16:1983–93.
[30] Guo Z, Park S, Hahn HT, Nanocomposite fabrication through particle surface initiated polymerization, AICHE Annual Meeting 2006; San Francisco.
[31] Stevens R. Defects in silicon carbide. J Mater Sci 1972;7:517–21.
[32] Cho E-C, Green MA, Xia J, Corkish R. Evidence for crystalline silicon oxide growth on thin silicon, in: Proc of COMMAD 2002, Conference on Optoelectronic and Microelectronic Materials and Devices 2002, pp. 421–4.
[33] Cho E-C, Green MA, Xia J, Corkish R, Reece P, Gal M. Clear quantum-confined luminescence from crystalline silicon/SiO_2 single quantum wells. Appl Phys Lett 2004;84:2286–8.
[34] Yong V. Nano-particulate dispersion and reinforcement of nano-structured composite materials. Phd thesis, 2005. University of California, Los Angeles.
[35] Chen Q, Xu R, Yu D. Multiwalled carbon nanotube/polybenzoxazine nanocomposites: Preparation, characterization and properties. Polymer 2006;47:7711–9.
[36] Rodgers RM, Mahfuz H, Rangari VK, Chisholm N, Jeelani S. Infusion of SiC nanoparticles into SC-15 epoxy: an investigation of thermal and mechanical response. Macromol Mater Eng 2005;290:423–9.
[37] Guo Z, Park S, Hahn HT, Wei S, Moldovan M, Karki AB, et al. Giant magnetoresistance behavior of an iron/carbonized polyurethane nanocomposite. Appl Phys Lett 2007;90:053111.
[38] Guo Z, Park S, Karki A, Young D, Hahn HT. Magnetic and electromagnetic evaluation of the magnetic nanoparticle filled polyurethane nanocomposites, in: Proc of 10th Joint MMM/Intermag Conf 2007, Baltimore, Maryland.